Available online at www.sciencedirect.com
SCIENCE DIRECT®
Journal of Sound and Vibration 266 (2003) 325–354
JOURNAL OF SOUND AND VIBRATION
www.elsevier.com/locate/jsvi

Non-linear responses of suspended cables to primary resonance excitations

H.N. Arafat, A.H. Nayfeh*

Department of Engineering Science and Mechanics, (MC 0219), Virginia Polytechnic Institute and State University, Blacksburg, VA 24061, USA

Received 19 February 2002; accepted 17 September 2002

Abstract

We investigate the non-linear forced responses of shallow suspended cables. We consider the following cases: (1) primary resonance of a single in-plane mode and (2) primary resonance of a single out-of-plane mode. In both cases, we assume that the excited mode is not involved in an autoparametric resonance with any other mode. We analyze the system by following two approaches. In the first, we discretize the equations of motion using the Galerkin procedure and then apply the method of multiple scales to the resulting system of non-linear ordinary-differential equations to obtain approximate solutions (discretization approach). In the second, we apply the method of multiple scales directly to the non-linear integral-partial-differential equations of motion and associated boundary conditions to determine approximate solutions (direct approach). We then compare results obtained with both approaches and discuss the influence of the number of modes retained in the discretization procedure on the predicted solutions.

1. Introduction

Suspended cables are key components in many mechanical systems and civil structures, and therefore understanding their behaviors under different load conditions is of great importance to engineers. In general, analytical solutions of non-linear systems are very scarce and often computational methods are required to determine the responses of such systems. When the non-linearity is "weak", asymptotic methods can be used to determine approximate analytical solutions of the system responses. These solutions, although not exact, are important because they can give general information about the system behavior for different parameter values.

*Corresponding author. Tel.: +1-540-231-5453; fax: +1-540-231-2290.
E-mail address: anayfeh@vt.edu (A.H. Nayfeh).

0022-460X/03/$ - see front matter
doi:10.1016/S0022-460X(02)01393-7

There are two popular approaches to calculating approximate analytical solutions of weakly non-linear distributed-parameter systems. In the first, the equations of motion are discretized by using a weighted-residual technique, and then the resulting non-linear ordinary-differential set of equations is solved using an asymptotic technique. In the second, solutions are calculated by applying an asymptotic technique directly to the governing partial-differential system and associated boundary conditions.

A common practice among many researchers who use the first approach is to perform the discretization by using a single mode or, when autoparametric resonances are present, a few modes. By means of several examples, Nayfeh and coworkers [1–8] have demonstrated that this reduced-order discretization approach can yield incorrect results. Pakdemirli and Boyaci [9] further investigated this problem for a general distributed-parameter system with quadratic and cubic non-linearities.

The forced planar dynamics of suspended cables near primary resonance were investigated by Benedettini and Rega [10]. They used a single-mode Galerkin discretization and then applied the method of multiple scales to calculate a fourth order asymptotic expansion of the solution. They found out that the response may be either hardening or softening, depending on the amplitude of oscillation. Rega et al. [7] investigated the primary resonance of the first in-plane mode of a suspended cable. They considered both the discretization and direct approaches and found that, when only a few number of modes is used in the reduced-order model, the results of the two approaches tend to deviate from each other. The out-of-plane oscillations of suspended cables to in-plane excitations were considered by Takahashi and Konishi [11]. They used a full-basis Galerkin discretization and then applied the method of harmonic balance to investigate regions of instability for several principal parametric and combination parametric resonances.

In this work, we use the method of multiple scales to investigate the responses of suspended cables to primary resonance excitations. We present analyses for both the direct and discretization approaches. We consider cases where the directly excited mode (be it in-plane or out-of-plane) is not involved in an autoparametric resonance with other modes. We then compare results of both approaches and explore the consequences of using only a few number of modes in the Galerkin discretization.

2. Problem formulation

Taking the cable span l as the characteristic length and $t^* = l/2\pi\sqrt{m/H}$ as the characteristic time, we express the non-dimensional non-planar equations of motion for a shallow suspended elastic cable (see Fig. 1) as [12,13]

$$\ddot{u}_1 + 2c_1\dot{u}_1 - u_1'' = \alpha(u_1'' + by'') \int_0^1 \left[by'u_1' + \frac{1}{2}(u_1'^2 + u_2'^2)\right] \mathrm{d}x + f_1(t), \tag{1}$$

$$\ddot{u}_2 + 2c_2\dot{u}_2 - u_2'' = \alpha u_2'' \int_0^1 \left[by'u_1' + \frac{1}{2}(u_1'^2 + u_2'^2)\right] \mathrm{d}x + f_2(t), \tag{2}$$

where $y(x) = -4x(1-x)$ and the boundary conditions are

$$u_1 = u_2 = 0 \quad \text{at } x = 0 \quad \text{and} \quad x = 1. \tag{3}$$

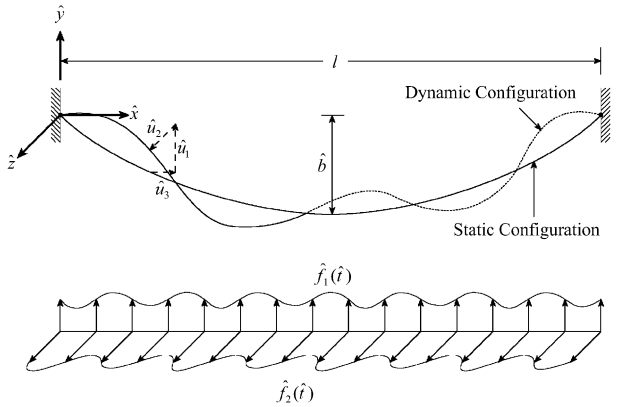

Fig. 1. A schematic of a suspended cable under external excitations.

The overdot and prime indicate the derivatives with respect to the non-dimensional time t and position x, respectively, $u_1(x,t)$ and $u_2(x,t)$ denote the non-dimensional in-plane and out-of-plane displacements, m is the mass per unit length, b the non-dimensional cable sag, E is Young's modulus, A the cross-sectional area, the c_i are the non-dimensional viscous damping coefficients, the $f_i(t)$ are the non-dimensional external excitations, g is acceleration due to gravity, H the horizontal component of the cable tension, and

$$\alpha = \frac{EA}{H} = \frac{8bEA}{mgl}. \tag{4}$$

Dropping the forcing, damping, and non-linear terms in Eqs. (1) and (2), we obtain the linearized equations of motion:

$$\ddot{u}_1 - u_1'' = \alpha b y'' \int_0^1 b y' u_1' \, \mathrm{d}x, \tag{5}$$

$$\ddot{u}_2 - u_2'' = 0. \tag{6}$$

Solving Eqs. (3), (5), and (6), we determine the mode shapes and natural frequencies of the cable [14]. For the *out-of-plane* motion, the nth mode shape and corresponding natural frequency are given by

$$\psi_n(x) = \sqrt{2}\sin(\lambda_n x) \quad \text{and} \quad \lambda_n = n\pi, \quad n = 1, 2, 3, \ldots, \tag{7}$$

where the mode shape is normalized so that $\int_0^1 \psi_n^2 \, \mathrm{d}x = 1$. For the *in-plane* motion, the nth *antisymmetric* (n = even) mode shape and corresponding natural frequency are given by

$$\phi_n(x) = \sqrt{2}\sin(\omega_n x) \quad \text{and} \quad \omega_n = n\pi, \tag{8}$$

and the nth *symmetric* (n = odd) mode shape is given by

$$\phi_n(x) = \kappa_n \left[1 - \cos(\omega_n x) - \tan\left(\frac{\omega_n}{2}\right)\sin(\omega_n x)\right]. \tag{9}$$

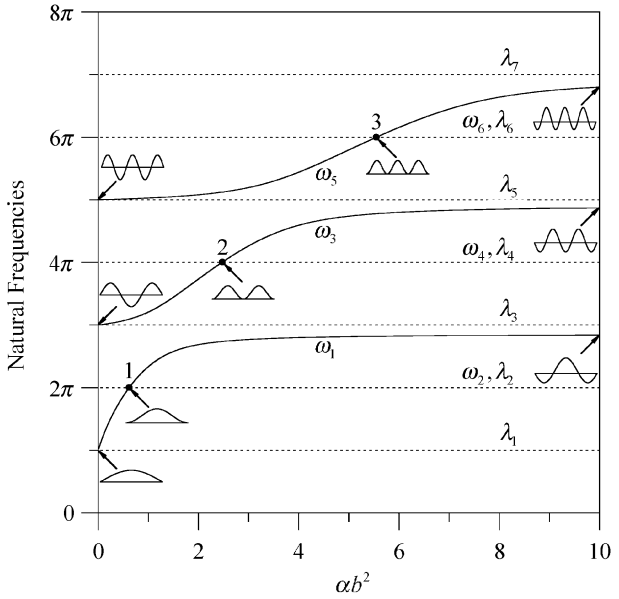

Fig. 2. Variation of the first few non-dimensional natural frequencies and mode shapes with αb^2.

The corresponding natural frequency ω_n is determined from

$$\tan\left(\frac{\omega_n}{2}\right) = \left(\frac{\omega_n}{2}\right) - \frac{1}{16\alpha b^2}\left(\frac{\omega_n}{2}\right)^3 \tag{10}$$

and κ_n is chosen such that $\int_0^1 \phi_n^2(x)\,\mathrm{d}x = 1$, yielding

$$\kappa_n = \sqrt{\frac{2\omega_n \cos^2(\omega_n/2)}{(2+\cos\omega_n)\omega_n - 3\sin\omega_n}}. \tag{11}$$

From Eq. (10), we note that the natural frequencies of the symmetric in-plane modes vary with αb^2. This results in the crossover points $\alpha b_n^2 = (n\pi)^2/16$, $n = 1, 2, 3, \ldots$, where the one-to-one and two-to-one autoparametric resonances $\omega_{2n-1} \approx 2\lambda_n = \omega_{2n} = \lambda_{2n}$ occur simultaneously. In Fig. 2, we present the first few natural frequencies as functions of αb^2 and indicate the first three crossover points.

3. Galerkin discretization procedure

To analyze the non-linear responses of this system, we first discretize Eqs. (1) and (2) using the mode shapes of the linearized problem. To this end, we express the in-plane and out-of-plane displacements u_1 and u_2 as

$$u_1(x,t) = \sum_{n=1}^{\infty} \phi_n(x)\eta_n(t), \tag{12}$$

$$u_2(x,t) = \sum_{n=1}^{\infty} \psi_n(x)\zeta_n(t), \tag{13}$$

where the $\eta_n(t)$ and $\zeta_n(t)$ are generalized co-ordinates. Next, we substitute Eqs. (12) and (13) into Eqs. (1) and (2), multiply, respectively, by the mode shape functions $\phi_k(x)$ and $\psi_l(x)$, integrate the outcomes over $x\in[0,1]$, and obtain the following system of non-linear ordinary-differential equations for the $\eta_k(t)$ and $\zeta_l(t)$:

$$\begin{aligned}\ddot{\eta}_k + 2\mu_{1k}\dot{\eta}_k + \omega_k^2\eta_k = {} & \frac{\alpha b}{2}\sum_{n=1}^{\infty}\sum_{r=1}^{\infty}[(U_kP_{nr} + 2P_{kn}U_r)\eta_n\eta_r] \\ & + \frac{\alpha b}{2}\sum_{n=1}^{\infty}\sum_{r=1}^{\infty}[(U_kQ_{nr})\zeta_n\zeta_r] - \frac{\alpha}{2}\sum_{n=1}^{\infty}\sum_{r=1}^{\infty}\sum_{j=1}^{\infty}[(P_{kn}P_{rj})\eta_n\eta_r\eta_j] \\ & - \frac{\alpha}{2}\sum_{n=1}^{\infty}\sum_{r=1}^{\infty}\sum_{j=1}^{\infty}[(P_{kn}Q_{rj})\eta_n\zeta_r\zeta_j] + f_{1k}(t).\end{aligned} \tag{14}$$

$$\begin{aligned}\ddot{\zeta}_l + 2\mu_{2l}\dot{\zeta}_l + \lambda_l^2\zeta_l = {} & \alpha b\sum_{n=1}^{\infty}\sum_{r=1}^{\infty}[(Q_{ln}U_r)\zeta_n\eta_r] - \frac{\alpha}{2}\sum_{n=1}^{\infty}\sum_{r=1}^{\infty}\sum_{j=1}^{\infty}[(Q_{ln}P_{rj})\zeta_n\eta_r\eta_j] \\ & - \frac{\alpha}{2}\sum_{n=1}^{\infty}\sum_{r=1}^{\infty}\sum_{j=1}^{\infty}[(Q_{ln}Q_{rj})\zeta_n\zeta_r\zeta_j] + f_{2l}(t),\end{aligned} \tag{15}$$

where $k,l = 1,2,3,\ldots$, $\mu_{1k} = \int_0^1 c_1\phi_k^2\,\mathrm{d}x$, $\mu_{2l} = \int_0^1 c_2\psi_l^2\,\mathrm{d}x$, and

$$U_n = \int_0^1 \phi_n y''\,\mathrm{d}x = -\int_0^1 \phi_n' y'\,\mathrm{d}x = \begin{cases} \dfrac{\kappa_n\omega_n^2}{8\alpha b^2} & \text{for } n = \text{odd}, \\ 0 & \text{for } n = \text{even}; \end{cases} \tag{16}$$

$$\begin{aligned} P_{rj} &= \int_0^1 \phi_r'\phi_j'\,\mathrm{d}x = -\int_0^1 \phi_r''\phi_j\,\mathrm{d}x \\ &= \begin{cases} -\dfrac{\kappa_r\kappa_j\omega_r^2\omega_j^2}{64\alpha b^2} & \text{for } r,j = \text{odd, and } r\neq j, \\ \dfrac{\kappa_r^2\omega_r(\omega_r - \sin\omega_r)}{2\cos^2(\frac{\omega_r}{2})} & \text{for } r = j = \text{odd}, \\ 0 & \text{for } r,j = \text{even and } r\neq j, \\ \omega_r^2 & \text{for } r = j = \text{even}, \\ 0 & \text{for } r = \text{odd, } j = \text{even and vice versa}; \end{cases} \end{aligned} \tag{17}$$

$$Q_{rj} = \int_0^1 \psi_r'\psi_j'\,\mathrm{d}x = -\int_0^1 \psi_r''\psi_j\,\mathrm{d}x = \begin{cases} \lambda_r^2 & \text{for } \forall r = j, \\ 0 & \text{for } \forall r,j \text{ and } r\neq j; \end{cases} \tag{18}$$

$$f_{1n}(t) = f_1(t)\int_0^1 \phi_n \,\mathrm{d}x = \begin{cases} \dfrac{\kappa_n \omega_n^2}{64\alpha b^2} f_1(t) & \text{for } n = \text{odd}, \\ 0 & \text{for } n = \text{even}; \end{cases} \tag{19}$$

$$f_{2n}(t) = f_2(t)\int_0^1 \psi_n \,\mathrm{d}x = \begin{cases} \dfrac{2\sqrt{2}}{\lambda_n} f_2(t) & \text{for } n = \text{odd}, \\ 0 & \text{for } n = \text{even}. \end{cases} \tag{20}$$

Eqs. (14) and (15) constitute two infinite sets of non-linearly coupled ordinary-differential equations that describe the non-planar dynamical behavior of the cable. For all practical purposes, one usually truncates Eqs. (14) and (15) by considering the contributions from K in-plane modes and L out-of-plane modes. This reduces the problem to solving a set of $K + L$ non-linear equations. The values of K and L are usually chosen by trial and error and are verified by testing the convergence of the solutions.

When a specific mode is directly excited and if it is not involved in an autoparametric resonance with any other mode, it is common practice to employ a single-mode discretization. That is, if the mth in-plane mode is the only one being excited, then one lets $u_2(x,t) = 0$ and $u_1(x,t) = \phi_m(x)\eta_m(t)$ in Eq. (1) and obtains the following equation for $\eta_m(t)$:

$$\ddot{\eta}_m + 2\mu_{1m}\dot{\eta}_m + \omega_m^2\eta_m = \tfrac{3}{2}\alpha b U_m P_{mm}\eta_m^2 - \tfrac{1}{2}\alpha P_{mm}^2\eta_m^3 + f_{1m}(t). \tag{21}$$

Similarly, if the sth out-of-plane mode is the only one being excited, then one lets $u_1(x,t) = 0$ and $u_2(x,t) = \psi_s(x)\zeta_s(t)$ in Eq. (2) and obtains the following equation for $\zeta_s(t)$:

$$\ddot{\zeta}_s + 2\mu_{2s}\dot{\zeta}_s + \lambda_s^2\zeta_s = -\tfrac{1}{2}\alpha Q_{ss}^2\zeta_s^3 + f_{2s}(t). \tag{22}$$

The questions we wish to answer here are: how much do the neglected modes contribute to the cable response? How do the solutions of the discretized system compare with the solutions obtained by directly attacking the original integral-partial-differential system?

4. Method of multiple scales

In order to answer these questions, we next seek solutions of this weakly non-linear system by using perturbation techniques [15]. In particular, we use the method of multiple scales to conduct the analyses. Two approaches are discussed and compared: (1) solving the original integral-partial-differential system directly and (2) solving the discretized system. In this section, we present the basis for both approaches and in Sections 5 and 6, we solve the specific cases of primary resonance of an in-plane mode and primary resonance of an out-of-plane mode, respectively.

4.1. Solving the partial-differential system directly: "direct approach"

To apply the method of multiple scales, we introduce the non-dimensional parameter $\varepsilon \ll 1$ for bookkeeping purposes and define the fast time scale $T_0 = t$ and the slow time scales $T_1 = \varepsilon t$

and $T_2 = \varepsilon^2 t$. Consequently, the first and second derivatives with respect to time are

$$\frac{\mathrm{d}}{\mathrm{d}t} = D_0 + \varepsilon D_1 + \varepsilon^2 D_2 + \cdots, \quad \frac{\mathrm{d}^2}{\mathrm{d}t^2} = D_0^2 + 2\varepsilon D_0 D_1 + \varepsilon^2 (D_1^2 + 2D_0 D_2) + \cdots, \tag{23}$$

where $D_n \equiv \partial/\partial T_n$. In addition, we scale the damping and forcing terms so that their influence balances the influence of the non-linearities. Hence, we set $c_j \to \varepsilon^2 c_j$ and $f_j(t) \to \varepsilon^3 f_j(t)$ in Eqs. (1) and (2). Next, we express the displacements as

$$u_1(x,t) = \varepsilon u_{11}(x, T_0, T_1, T_2) + \varepsilon^2 u_{12}(x, T_0, T_1, T_2) + \varepsilon^3 u_{13}(x, T_0, T_1, T_2) + \cdots, \tag{24}$$

$$u_2(x,t) = \varepsilon u_{21}(x, T_0, T_1, T_2) + \varepsilon^2 u_{22}(x, T_0, T_1, T_2) + \varepsilon^3 u_{23}(x, T_0, T_1, T_2) + \cdots, \tag{25}$$

in Eqs. (1)–(3), use Eqs. (23), separate terms of equal powers in ε, and obtain:

Order ε:

$$D_0^2 u_{11} - u_{11}'' - \alpha b^2 y'' \int_0^1 y' u_{11}' \,\mathrm{d}x = 0, \tag{26}$$

$$D_0^2 u_{21} - u_{21}'' = 0. \tag{27}$$

Order ε^2:

$$\begin{aligned} D_0^2 u_{12} - u_{12}'' - \alpha b^2 y'' \int_0^1 y' u_{12}' \,\mathrm{d}x = & -2D_0 D_1 u_{11} + \alpha b u_{11}'' \int_0^1 y' u_{11}' \,\mathrm{d}x \\ & + \frac{1}{2}\alpha b y'' \int_0^1 u_{11}'^2 \,\mathrm{d}x + \frac{1}{2}\alpha b y'' \int_0^1 u_{21}'^2 \,\mathrm{d}x, \end{aligned} \tag{28}$$

$$D_0^2 u_{22} - u_{22}'' = -2D_0 D_1 u_{21} + \alpha b u_{21}'' \int_0^1 y' u_{11}' \,\mathrm{d}x. \tag{29}$$

Order ε^3:

$$\begin{aligned} D_0^2 u_{13} - u_{13}'' - \alpha b^2 y'' \int_0^1 y' u_{13}' \,\mathrm{d}x = & -D_1^2 u_{11} - 2D_0 D_2 u_{11} - 2D_0 D_1 u_{12} - 2c_1 D_0 u_{11} \\ & + \alpha b u_{11}'' \int_0^1 y' u_{12}' \,\mathrm{d}x + \alpha b u_{12}'' \int_0^1 y' u_{11}' \,\mathrm{d}x \\ & + \frac{1}{2}\alpha u_{11}'' \int_0^1 u_{11}'^2 \,\mathrm{d}x + \alpha b y'' \int_0^1 u_{11}' u_{12}' \,\mathrm{d}x \\ & + \frac{1}{2}\alpha u_{11}'' \int_0^1 u_{21}'^2 \,\mathrm{d}x + \alpha b y'' \int_0^1 u_{21}' u_{22}' \,\mathrm{d}x \\ & + f_1(T_0), \end{aligned} \tag{30}$$

$$D_0^2 u_{23} - u_{23}'' = -D_1^2 u_{21} - 2D_0 D_2 u_{21} - 2D_0 D_1 u_{22} - 2c_2 D_0 u_{21} + \alpha b u_{21}'' \int_0^1 y' u_{12}' \, \mathrm{d}x + \alpha b u_{22}'' \int_0^1 y' u_{11}' \, \mathrm{d}x + \frac{1}{2}\alpha u_{21}'' \int_0^1 u_{11}'^2 \, \mathrm{d}x + \frac{1}{2}\alpha u_{21}'' \int_0^1 u_{21}'^2 \, \mathrm{d}x + f_2(T_0). \tag{31}$$

The equations are subject to the boundary conditions

$$u_{jk}(0, T_0, T_1, T_2) = u_{jk}(1, T_0, T_1, T_2) = 0, \quad j, k = 1, 2, 3. \tag{32}$$

The general solutions of Eqs. (26), (27), and (32) can be expressed as

$$u_{11}(x, T_0, T_1, T_2) = \sum_{k=1}^{\infty} \phi_k(x)[A_k(T_1, T_2)\mathrm{e}^{\mathrm{i}\omega_k T_0} + \bar{A}_k(T_1, T_2)\mathrm{e}^{-\mathrm{i}\omega_k T_0}], \tag{33}$$

$$u_{21}(x, T_0, T_1, T_2) = \sum_{l=1}^{\infty} \psi_l(x)[B_l(T_1, T_2)\mathrm{e}^{\mathrm{i}\lambda_l T_0} + \bar{B}_l(T_1, T_2)\mathrm{e}^{-\mathrm{i}\lambda_l T_0}], \tag{34}$$

where the $\phi_k(x)$ and $\psi_l(x)$ are the linear mode shapes, defined by Eqs. (7)–(9), the ω_k and λ_l are the corresponding natural frequencies, the A_k and B_l are slowly time-varying complex-valued functions, and the $\bar{A}_k$ and $\bar{B}_l$ are their complex conjugates. In terms of real-valued amplitude and phase functions,

$$A_k(T_1, T_2) = \tfrac{1}{2} a_k(T_1, T_2)\mathrm{e}^{\mathrm{i}\beta_k(T_1, T_2)} \quad \text{and} \quad B_l(T_1, T_2) = \tfrac{1}{2}\hat{a}_l(T_1, T_2)\mathrm{e}^{\mathrm{i}\hat{\beta}_l(T_1, T_2)}. \tag{35}$$

4.2. Solving the discretized system: "discretization approach"

Using the previously defined time scales and bookkeeping parameter ε, we express the generalized co-ordinates $\eta_k(t)$ and $\zeta_l(t)$ as

$$\eta_k(t; \varepsilon) = \varepsilon\eta_{k1}(T_0, T_1, T_2) + \varepsilon^2\eta_{k2}(T_0, T_1, T_2) + \varepsilon^3\eta_{k3}(T_0, T_1, T_2) + \cdots, \tag{36}$$

$$\zeta_l(t; \varepsilon) = \varepsilon\zeta_{l1}(T_0, T_1, T_2) + \varepsilon^2\zeta_{l2}(T_0, T_1, T_2) + \varepsilon^3\zeta_{l3}(T_0, T_1, T_2) + \cdots \tag{37}$$

in Eqs. (14) and (15). Then, we use Eqs. (23), set $\mu_{jk} \to \varepsilon^2\mu_{jk}$ and $f_{jk}(t) \to \varepsilon^3 f_{jk}(t)$, separate terms of equal powers of ε, and obtain the following:

Order ε:

$$D_0^2\eta_{k1} + \omega_k^2\eta_{k1} = 0, \tag{38}$$

$$D_0^2\zeta_{l1} + \lambda_l^2\zeta_{l1} = 0. \tag{39}$$

Order ε^2:

$$D_0^2\eta_{k2} + \omega_k^2\eta_{k2} = -2D_0D_1\eta_{k1} + \frac{1}{2}\alpha b\sum_{n=1}^{\infty}\sum_{r=1}^{\infty}[(U_kQ_{nr})\zeta_{n1}\zeta_{r1}] + \frac{1}{2}\alpha b\sum_{n=1}^{\infty}\sum_{r=1}^{\infty}[(U_kP_{nr} + 2P_{kn}U_r)\eta_{n1}\eta_{r1}], \tag{40}$$

$$D_0^2\zeta_{l2} + \lambda_l^2\zeta_{l2} = -2D_0D_1\zeta_{l1} + \alpha b\sum_{n=1}^{\infty}\sum_{r=1}^{\infty}[(Q_{ln}U_r)\zeta_{n1}\eta_{r1}]. \tag{41}$$

Order ε^3:

$$\begin{aligned} D_0^2\eta_{k3} + \omega_k^2\eta_{k3} = &-D_1^2\eta_{k1} - 2D_0D_2\eta_{k1} - 2D_0D_1\eta_{k2} - 2\mu_{1k}D_0\eta_{k1} \\ &+ \frac{1}{2}\alpha b\sum_{n=1}^{\infty}\sum_{r=1}^{\infty}[(U_kP_{nr} + 2P_{kn}U_r)(\eta_{n1}\eta_{r2} + \eta_{n2}\eta_{r1})] \\ &+ \frac{1}{2}\alpha b\sum_{n=1}^{\infty}\sum_{r=1}^{\infty}[(U_kQ_{nr})(\zeta_{n1}\zeta_{r2} + \zeta_{n2}\zeta_{r1})] \\ &- \frac{1}{2}\alpha\sum_{n=1}^{\infty}\sum_{r=1}^{\infty}\sum_{j=1}^{\infty}[(P_{kn}P_{rj})\eta_{n1}\eta_{r1}\eta_{j1}] \\ &- \frac{1}{2}\alpha\sum_{n=1}^{\infty}\sum_{r=1}^{\infty}\sum_{j=1}^{\infty}[(P_{kn}Q_{rj})\eta_{n1}\zeta_{r1}\zeta_{j1}] + f_{1k}(T_0), \end{aligned} \tag{42}$$

$$\begin{aligned} D_0^2\zeta_{l3} + \lambda_l^2\zeta_{l3} = &-D_1^2\zeta_{l1} - 2D_0D_2\zeta_{l1} - 2D_0D_1\zeta_{l2} - 2\mu_{2l}D_0\zeta_{l1} \\ &+ \alpha b\sum_{n=1}^{\infty}\sum_{r=1}^{\infty}[(Q_{ln}U_r)(\zeta_{n1}\eta_{r2} + \zeta_{n2}\eta_{r1})] \\ &- \frac{1}{2}\alpha\sum_{n=1}^{\infty}\sum_{r=1}^{\infty}\sum_{j=1}^{\infty}[(Q_{ln}P_{rj})\zeta_{n1}\eta_{r1}\eta_{j1}] \\ &- \frac{1}{2}\alpha\sum_{n=1}^{\infty}\sum_{r=1}^{\infty}\sum_{j=1}^{\infty}[(Q_{ln}Q_{rj})\zeta_{n1}\zeta_{r1}\zeta_{j1}] + f_{2l}(T_0). \end{aligned} \tag{43}$$

The general solutions of Eqs. (38) and (39) can be expressed as

$$\eta_{k1}(T_0, T_1, T_2) = A_k(T_1, T_2)e^{i\omega_kT_0} + cc \quad \forall k, \tag{44}$$

$$\zeta_{l1}(T_0, T_1, T_2) = B_l(T_1, T_2)e^{i\lambda_lT_0} + cc \quad \forall l. \tag{45}$$

where *cc* stands for the complex conjugate of the preceding terms.

5. Primary resonance of an in-plane mode

We consider here the cable's response when the mth in-plane mode is excited near primary resonance. Because we are assuming that the mth mode is not involved in an autoparametric resonance with any of the other modes and since damping is present in the system, the free responses of the rest of the modes are assumed to die out after a long time [16].

5.1. Direct approach

In this case, we set

$$u_{11}(x, T_0, T_1, T_2) = \phi_m(x)[A_m(T_1, T_2)\mathrm{e}^{\mathrm{i}\omega_m T_0} + \bar{A}_m(T_1, T_2)\mathrm{e}^{-\mathrm{i}\omega_m T_0}], \tag{46}$$

$$u_{21}(x, T_0, T_1, T_2) = 0, \tag{47}$$

$$f_1(T_0) = F_1\cos(\Omega T_0), \quad f_2(T_0) = 0 \tag{48, 49}$$

and introduce the detuning parameter σ such that

$$\Omega = \omega_m + \varepsilon^2\sigma. \tag{50}$$

Substituting Eq. (47) into Eqs. (29) and (31), we find that $u_{22} = 0$ and $u_{23} = 0$, and therefore the out-of-plane displacement $u_2(x, t) = 0$. Next, we substitute Eq. (46) into Eq. (28), use Eqs. (16) and (17), and obtain

$$D_0^2 u_{12} - u_{12}'' - \alpha b^2 y'' \int_0^1 y' u_{12}'\,\mathrm{d}x = \alpha b\left(\frac{1}{2}y'' P_{mm} - \phi_m'' U_m\right)[(A_m^2\mathrm{e}^{2\mathrm{i}\omega_m T_0} + cc) + 2A_m\bar{A}_m] - 2\mathrm{i}\omega_m\phi_m\left(\frac{\partial A_m}{\partial T_1}\mathrm{e}^{\mathrm{i}\omega_m T_0} + cc\right). \tag{51}$$

To avoid the presence of secular terms in the solution, we need to set $\partial A_m/\partial T_1 = 0$; that is, $A_m = A_m(T_2)$ only. Consequently, the solution of Eq. (51) is given by

$$u_{12}(x, T_0, T_2) = G_1(x)(A_m^2\mathrm{e}^{2\mathrm{i}\omega_m T_0} + cc) + G_2(x)A_m\bar{A}_m, \tag{52}$$

where $G_1(x)$ and $G_2(x)$ are governed by the following boundary-value problems:

$$G_1'' + 4\omega_m^2 G_1 + \alpha b^2 y'' \int_0^1 y' G_1'\,\mathrm{d}x = -\alpha b\left(\frac{1}{2}y'' P_{mm} - U_m\phi_m''\right),$$
$$G_1(0) = G_1(1) = 0, \tag{53}$$

$$G_2'' + \alpha b^2 y'' \int_0^1 y' G_2'\,\mathrm{d}x = -2\alpha b\left(\frac{1}{2}y'' P_{mm} - U_m\phi_m''\right),$$
$$G_2(0) = G_2(1) = 0. \tag{54}$$

In Appendix A, we present the solutions of Eqs. (53) and (54).

Next, we substitute Eqs. (46) and (52) into Eq. (30), use Eq. (50), and obtain

$$\begin{aligned} D_0^2 u_{13} - u_{13}'' - \alpha b^2 y'' \int_0^1 y' u_{13}' \,\mathrm{d}x \\ = \left\{ -2\mathrm{i}\omega_m \phi_m \left(\frac{\mathrm{d}A_m}{\mathrm{d}T_2} + c_1 A_m \right) + \frac{1}{2} F_1 \mathrm{e}^{\mathrm{i}\sigma T_2} \right. \\ + \alpha b \left[y'' \int_0^1 \phi_m' G_1' \,\mathrm{d}x + \phi_m'' \int_0^1 y' G_1' \,\mathrm{d}x \right. \\ + G_1'' \int_0^1 y' \phi_m' \,\mathrm{d}x + y'' \int_0^1 \phi_m' G_2' \,\mathrm{d}x \\ \left. + \phi_m'' \int_0^1 y' G_2' \,\mathrm{d}x + G_2'' \int_0^1 y' \phi_m' \,\mathrm{d}x \right] A_m^2 \bar{A}_m \\ \left. + \frac{3}{2} \alpha \left(\phi_m'' \int_0^1 \phi_m'^2 \,\mathrm{d}x \right) A_m^2 \bar{A}_m \right\} \mathrm{e}^{\mathrm{i}\omega_m T_0} + cc + NST \\ \equiv \mathscr{G}(x, T_2) \mathrm{e}^{\mathrm{i}\omega_m T_0} + cc + NST, \end{aligned} \tag{55}$$

where NST stands for the terms that do not produce secular terms. Then, letting

$$u_{13}(x, T_0, T_2) = G_3(x, T_2) \mathrm{e}^{\mathrm{i}\omega_m T_0} + cc + NST \tag{56}$$

in Eq. (55), we obtain

$$\frac{\partial^2 G_3}{\partial x^2} + \omega_m^2 G_3 + \alpha b^2 y'' \int_0^1 y' \frac{\partial G_3}{\partial x} \,\mathrm{d}x = -\mathscr{G}(x, T_2), \quad G_3(0) = G_3(1) = 0. \tag{57}$$

The homogeneous problem in Eq. (57) has non-trivial solutions. Therefore, the non-homogeneous problem has solutions provided that a solvability condition is met. To determine this condition, we multiply Eq. (57) by the adjoint function $g_3(x)$, integrate the outcome by parts from $x = 0$ to 1, and obtain

$$\begin{aligned} \left[g_3 \frac{\partial G_3}{\partial x} - \alpha b^2 y' g_3 \int_0^1 y'' G_3 \,\mathrm{d}x \right]_0^1 + \int_0^1 G_3 \left[g_3'' + \omega_m^2 g_3 + \alpha b^2 y'' \int_0^1 g_3' y' \,\mathrm{d}x \right] \mathrm{d}x \\ = - \int_0^1 g_3 \mathscr{G} \,\mathrm{d}x. \end{aligned} \tag{58}$$

The adjoint is determined by considering the homogeneous problem in Eq. (58), which is the same as the linear eigenvalue problem. Therefore, we find that $g_3(x) = \phi_m(x)$, and consequently Eq. (58) reduces to the solvability condition

$$\int_0^1 \phi_m(x) \mathscr{G}(x, T_2) \,\mathrm{d}x = 0. \tag{59}$$

Using Eqs. (16), (17), and (55), we obtain the following equation for $A_m(T_2)$:

$$2\mathrm{i}\omega_m \left(\frac{\mathrm{d}A_m}{\mathrm{d}T_2} + \mu_{1m} A_m \right) + \Gamma_{em}^* A_m^2 \bar{A}_m = \frac{1}{2} F_{1m} \mathrm{e}^{\mathrm{i}\sigma T_2}, \tag{60}$$

where $F_{1m} = F_1 \int_0^1 \phi_m \, dx$ and the coefficient Γ^*_{em} of the effective non-linearity for the mth in-plane mode is given by

$$\Gamma^*_{em} = \frac{3}{2}\alpha P^2_{mm} - \alpha b \int_0^1 [(2U_m\phi'_m - P_{mm}y')(G'_1 + G'_2)]\, dx. \tag{61}$$

When the mth in-plane mode is symmetric (m = odd), the final expression for Γ^*_{em} becomes

$$\begin{aligned}\Gamma^*_{em} = {} & \frac{3}{2}\alpha P^2_{mm} - 8\alpha^2 b^2 P^2_{mm}\left\{\frac{[(48\alpha b^2 + 3 - 2\omega_m^2)\omega_m \cos\omega_m - 3(16\alpha b^2 + 1)\sin\omega_m]}{\cos\omega_m(16\alpha b^2 + 3)[16\alpha b^2(\omega_m - \tan\omega_m) - \omega_m^3]}\right\} \\ & - \frac{1}{24}\alpha P_{mm} U_m \kappa_m \left\{64\alpha b^2 - \frac{(16\alpha b^2 - 33)\omega_m^2}{(16\alpha b^2 + 3)} - \frac{64\alpha b^2 \tan\omega_m}{\omega_m}\right. \\ & \left. + \frac{\sin^2(\frac{\omega_m}{2})(64\alpha b^2 - \omega_m^2)[16\alpha b^2(\omega_m - \tan\omega_m) + \omega_m^3]}{\cos\omega_m[16\alpha b^2(\omega_m - \tan\omega_m) - \omega_m^3]}\right\} \\ & - \frac{1}{288}\alpha\omega_m U_m^2 \kappa_m^2 \left\{\frac{480\alpha b^2\omega_m}{\cos^2(\frac{\omega_m}{2})} + \frac{\omega_m^2 \sin^4(\frac{\omega_m}{2})(64\alpha b^2 - \omega_m^2)^2}{\cos^2\omega_m[16\alpha b^2(\omega_m - \tan\omega_m) - \omega_m^3]}\right. \\ & \left. - \frac{54\omega_m^3}{(16\alpha b^2 + 3)} + \frac{(64\alpha b^2\omega_m - \omega_m^3)(4 - 19\cos\omega_m)}{2\cos\omega_m}\right\},\end{aligned} \tag{62}$$

where κ_m, U_m, and P_{mm} are defined by Eqs. (11), (16), and (17). On the other hand, when the mth mode is antisymmetric (m = even), $U_m = 0$ and the expression for Γ^*_{em} reduces to

$$\Gamma^*_{em} = \frac{3}{2}\alpha m^4\pi^4 - \frac{8\alpha^2 b^2 m^4\pi^4(48\alpha b^2 + 3 - 2m^2\pi^2)}{(16\alpha b^2 + 3)(16\alpha b^2 - m^2\pi^2)}. \tag{63}$$

Substituting the results obtained for the u_{jk} back into Eqs. (24) and (25), using Eq. (35), and setting $T_n = \varepsilon^n t$, the response of the system to second order in ε is given by $u_2(x,t) = O(\varepsilon^3)$ and

$$\begin{aligned}u_1(x,t) = {} & \varepsilon\phi_m(x) a_m \cos(\omega_m t + \beta_m) \\ & + \tfrac{1}{2}\varepsilon^2 a_m^2 [G_1(x)\cos(2\omega_m t + 2\beta_m) + \tfrac{1}{2}G_2(x)] + O(\varepsilon^3).\end{aligned} \tag{64}$$

We note that, by virtue of Eq. (10), as $\omega_m \to \omega_n/2$, the term $[16\alpha b^2(\omega_m - \tan\omega_m) - \omega_m^3] \to 0$ and Eq. (62) becomes singular. Moreover, Eq. (63) becomes singular when $\alpha b^2 \to m^2\pi^2/16$, which are the even crossover points (see Fig. 2); these correspond to the autoparametric resonances $\omega_{2m-1} \approx 2\omega_m$, $m = 2, 4, \ldots$. Resonance conditions such as the ones occurring in Eqs. (62) and (63) are clearly demonstrated in the results obtained by applying the discretization approach, as is presented next.

5.2. Discretization approach

In this case, we set

$$\eta_{m1} = A_m(T_1, T_2)e^{i\omega_m T_0} + cc, \tag{65}$$

$$\eta_{k1} = 0 \quad \forall k \neq m, \tag{66}$$

$$\zeta_{l1} = 0 \quad \forall l, \tag{67}$$

$$f_{1k}(T_0) = F_{1k}\cos(\Omega T_0) \quad \forall k, \tag{68}$$

$$f_{2l}(T_0) = 0 \quad \forall l, \tag{69}$$

where Ω is related to ω_m by Eq. (50). We substitute Eqs. (65)–(67) into Eqs. (40) and (41), determine that $\partial A_m/\partial T_1 = 0$, solve for the η_{k2} and ζ_{l2}, and obtain

$$\eta_{k2} = E_{1k}(A_m^2 e^{2i\omega_m T_0} + cc) + E_{2k}A_m\bar{A}_m \quad \forall k, \tag{70}$$

$$\zeta_{l2} = 0 \quad \forall l, \tag{71}$$

where

$$E_{1k} = \frac{1}{2}\alpha b\left(\frac{U_k P_{mm} + 2P_{km}U_m}{\omega_k^2 - 4\omega_m^2}\right) \quad \text{and} \quad E_{2k} = \alpha b\left(\frac{U_k P_{mm} + 2P_{km}U_m}{\omega_k^2}\right). \tag{72}$$

We note from Eqs. (70) and (72) that this solution breaks down when $\omega_k \approx 2\omega_m$, a two-to-one autoparametric resonance between two in-plane modes.

To determine $A_m(T_2)$, we set $k = m$ in Eq. (42), use Eqs. (66)–(68) and (71), and obtain

$$\begin{aligned} D_0^2\eta_{m3} + \omega_m^2\eta_{m3} = & -2D_0D_2\eta_{m1} - 2\mu_{1m}D_0\eta_{m1} \\ & + \frac{1}{2}\alpha b\sum_{r=1}^{\infty}[(U_m P_{mr} + 2P_{mm}U_r)\eta_{m1}\eta_{r2}] \\ & + \frac{1}{2}\alpha b\sum_{n=1}^{\infty}[(U_m P_{nm} + 2P_{mn}U_m)\eta_{m1}\eta_{n2}] \\ & - \frac{1}{2}\alpha P_{mm}^2\eta_{m1}^3 + F_{1m}\cos(\Omega T_0). \end{aligned} \tag{73}$$

Then, substituting for the η_{m1} and η_{k2} from Eqs. (65) and (70), using Eq. (50), and setting the terms that produce secular terms equal to zero, we obtain the following equation for $A_m(T_2)$:

$$2i\omega_m\left(\frac{dA_m}{dT_2} + \mu_{1m}A_m\right) + \Gamma_{em}A_m^2\bar{A}_m = \frac{1}{2}F_{1m}e^{i\sigma T_2}, \tag{74}$$

where the coefficient Γ_{em} of the effective non-linearity of the mth in-plane mode is given by

$$\Gamma_{em} = \frac{3}{2}\alpha P_{mm}^2 - \frac{1}{2}\alpha^2 b^2\sum_{r=1}^{\infty}\left\{(U_r P_{mm} + 2P_{rm}U_m)^2\left[\frac{3\omega_r^2 - 8\omega_m^2}{\omega_r^2(\omega_r^2 - 4\omega_m^2)}\right]\right\}. \tag{75}$$

If the mth mode is *symmetric* (i.e., $m =$ odd), then after substituting for the U_k and P_{rj}, we find that Eq. (75) becomes

$$\Gamma_{em} = \left(\frac{3}{2}\alpha - \frac{15\kappa_m^2\omega_m^2}{128b^2}\right)\frac{\kappa_m^4\omega_m^2(\omega_m - \sin\omega_m)^2}{4\cos^4(\frac{\omega_m}{2})} - \sum_{\substack{r=odd \\ r\neq m}}^{\infty}\left\{\frac{\kappa_r^2\kappa_m^4\omega_r^2\omega_m^2(3\omega_r^2 - 8\omega_m^2)}{524\,288\alpha^2b^6(\omega_r^2 - 4\omega_m^2)\cos^4(\frac{\omega_m}{2})} \times [32\alpha b^2\sin\omega_m - 32\alpha b^2\omega_m + (1+\cos\omega_m)\omega_m^3]^2\right\}. \tag{76}$$

On the other hand, if the mth mode is *antisymmetric* (i.e., $m =$ even), then Eq. (75) reduces to the expression

$$\Gamma_{em} = \frac{3}{2}\alpha m^4\pi^4 - \frac{m^4\pi^4}{128b^2}\sum_{r=odd}^{\infty}\left[\frac{\kappa_r^2\omega_r^2(3\omega_r^2 - 8m^2\pi^2)}{(\omega_r^2 - 4m^2\pi^2)}\right]. \tag{77}$$

Looking at the expressions for the effective non-linearities in Eqs. (76) and (77), we note that they consist of two parts. The first part is the effective non-linearity one would obtain if a single-mode discretization is used. The second part is the summation of the contributions of all of the other modes to the effective non-linearity of the mth mode. In this case, we note that only the symmetric modes contribute. Substituting the results obtained for the η_{kj} and ζ_{lj} back into Eqs. (36) and (37), using Eqs. (12), (13), and (35), and setting $T_n = \varepsilon^n t$, we obtain the system's response to second-order in ε as $u_2(x,t) = O(\varepsilon^3)$ and

$$u_1(x,t) = \varepsilon\phi_m(x)a_m\cos(\omega_m t + \beta_m) + \frac{1}{2}\varepsilon^2 a_m^2\sum_{r=odd}^{\infty}\left\{\phi_r(x)\left[E_{1r}\cos(2\omega_m t + 2\beta_m) + \frac{1}{2}E_{2r}\right]\right\} + O(\varepsilon^3). \tag{78}$$

Comparing Eqs. (64) and (78), we find that the solutions from both approaches are equivalent if $\sum_{r=odd}^{\infty} E_{1r}\phi_r(x) = G_1(x)$ and $\sum_{r=odd}^{\infty} E_{2r}\phi_r(x) = G_2(x)$, in agreement with the general results of Pakdemirli and Boyaci [9].

5.3. Results and comparison

When $\Gamma_{em}, \Gamma_{em}^* > 0$, the frequency–response curves are bent to the right and the effective non-linearity is of the "hardening" type. On the other hand, when $\Gamma_{em}, \Gamma_{em}^* < 0$, the frequency–response curves are bent to the left and the effective non-linearity is of the "softening" type [16].

As an example, we consider a cable for which $\alpha = 239.16$ and investigate the influence of the number of modes retained in Eqs. (76) and (77) on the value of the coefficient Γ_{em} of the effective non-linearity. These results are also compared to their corresponding values of Γ_{em}^*, evaluated

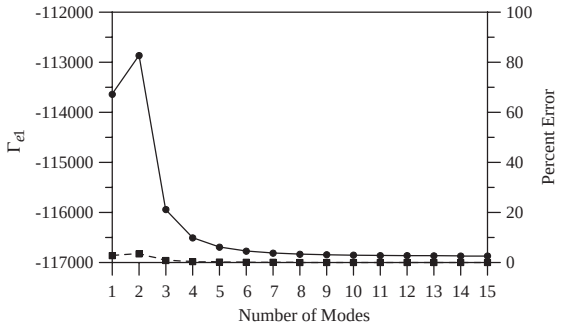

Fig. 3. The coefficient Γ_{e1} (—●—) of the effective non-linearity of the first symmetric in-plane mode ($m = 1$) and percent error (–▩–) as a function of the number of modes considered when $\alpha = 239.16$ and $\alpha b^2 = \frac{1}{2}$.

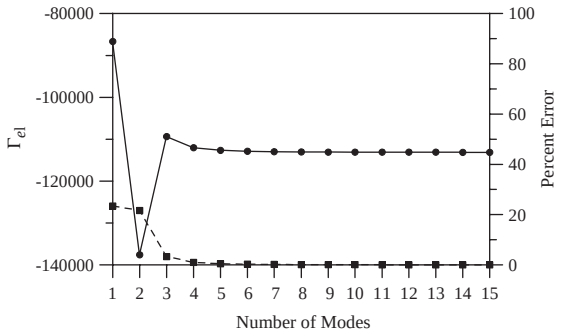

Fig. 4. The coefficient Γ_{e1} (—●—) of the effective non-linearity of the first symmetric in-plane mode ($m = 1$) and percent error (–▩–) as a function of the number of modes considered when $\alpha = 239.16$ and $\alpha b^2 = 2$.

from Eqs. (62) and (63), by calculating the percent errors:

$$E_{em} \equiv \left| \frac{(\Gamma^*_{em} - \Gamma_{em})}{\Gamma^*_{em}} \right| \times 100\%. \tag{79}$$

We consider the primary resonance of the first symmetric in-plane mode (i.e., $m = 1$) and the primary resonance of the first antisymmetric in-plane mode (i.e., $m = 2$). Because the natural frequencies of the symmetric in-plane modes vary as a function of αb^2, we present results for three cases: $\alpha b^2 = \frac{1}{2}$ (left of first crossover), $\alpha b^2 = 2$ (right of first crossover), and $\alpha b^2 = 4$ (right of second crossover). The corresponding values of the sag-to-span ratio $b = \hat{b}/l$ are approximately $\frac{1}{21.9}$, $\frac{1}{10.9}$, and $\frac{1}{7.7}$, respectively, which are acceptable for the "shallow" suspended cable theory [14].

5.3.1. First symmetric in-plane mode: $\Omega \approx \omega_1$

In Fig. 3, we present variation of Γ_{e1} and corresponding percent error when $\alpha b^2 = \frac{1}{2}$ (left of first crossover) with the number of modes retained in Eq. (76). Using a single-mode discretization, $\Gamma_{e1} = -113\,640.7$. If, instead, both modes 1 and 3 are used in the discretization, Γ_{e1} increases to $-112\,866.2$. As more modes are included in the discretization, Γ_{e1} monotonously converges onto

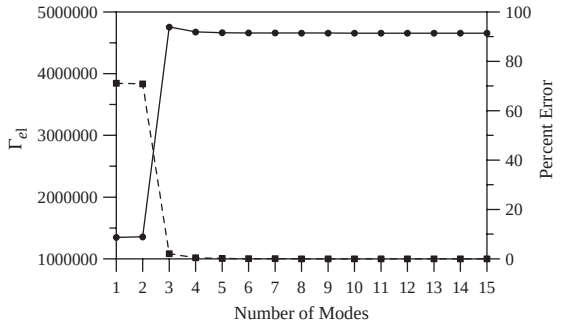

Fig. 5. The coefficient Γ_{e1} (—●—) of the effective non-linearity of the first symmetric in-plane mode ($m = 1$) and percent error (–▩–) as a function of the number of modes considered when $\alpha = 239.16$ and $\alpha b^2 = 4$.

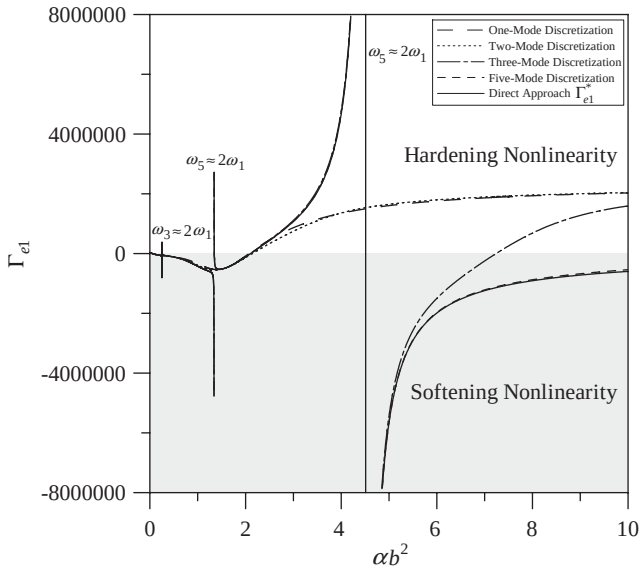

Fig. 6. The coefficient Γ_{e1} of the effective non-linearity of the first symmetric in-plane mode ($m = 1$) as a function of αb^2 when $\alpha = 239.16$.

the correct value. When 15 modes are retained in the discretization, $\Gamma_{e1} = -116\,871.7$. The value obtained by the direct approach is $\Gamma^*_{e1} = -116\,878.2$. The percent errors when using single-, two-, three-, and ten-mode discretizations are $E_{e1} = 2.8\%$, 3.4%, 0.8%, and 0.019%, respectively.

Choosing $\alpha b^2 = 2$ (right of first crossover), we present in Fig. 4 the variation of Γ_{e1} and the corresponding percent error with the number of modes retained. The value obtained by the direct approach is $\Gamma^*_{e1} = -113\,146.7$. Switching from a single-mode to a two-mode discretization, we find that Γ_{e1} jumps from $-86\,661.5$ to $-137\,601.1$, which is beyond the true value. In this case, the percent errors when using single-, two-, three-, and ten-mode discretizations are 23.4%, 21.6%, 3.3%, and 0.046%, respectively.

Lastly, we choose $\alpha b^2 = 4$ (right of second crossover) and present in Fig. 5 the variation of Γ_{e1} and the corresponding percent error with the number of modes retained. The value obtained by the direct approach is $\Gamma^*_{e1} = 4\,654\,599.6$. Using single- and two-mode discretizations, we find that the corresponding values of $\Gamma_{e1} = 1\,345\,575.9$ and $1\,356\,450.4$, which are relatively close to each other, but quite off the correct value. However, as we include more modes, a sharp jump in the value of Γ_{e1} occurs, and after 15 modes, Γ_{e1} converges to $4\,654\,795.8$. The percent errors when using single-, two-, three-, and ten-mode discretizations are 71.1%, 70.9%, 2.1%, and 0.02%.

From Figs. 3 and 4, we note that the final values of $\Gamma_{e1} < 0$, and therefore the effective non-linearity for the first symmetric in-plane mode for these two cases is softening. From Fig. 5, we note that the final value of $\Gamma_{e1} > 0$, indicating that for this case, the effective non-linearity of the first mode is hardening. Moreover, from Figs. 4 and 5, we find that using single- and two-mode discretizations results in significant quantitative errors.

In Fig. 6, we show the influence of αb^2 on Γ_{e1} when using the direct and discretization approaches; results for single-, two-, three-, and five-mode discretizations are presented. The results of Γ^*_{e1} from the direct approach contain several singularities corresponding to the autoparametric resonances $\omega_r \approx 2\omega_1$, $r = 3, 5, \ldots$. For $\alpha b^2 \in [0, 10]$, the resonance $\omega_3 \approx 2\omega_1$ occurs once, whereas the resonance $\omega_5 \approx 2\omega_1$ occurs twice. If one uses single-mode or two-mode discretizations, significant deviations between the values of Γ_{e1} and Γ^*_{e1} can occur. These errors are

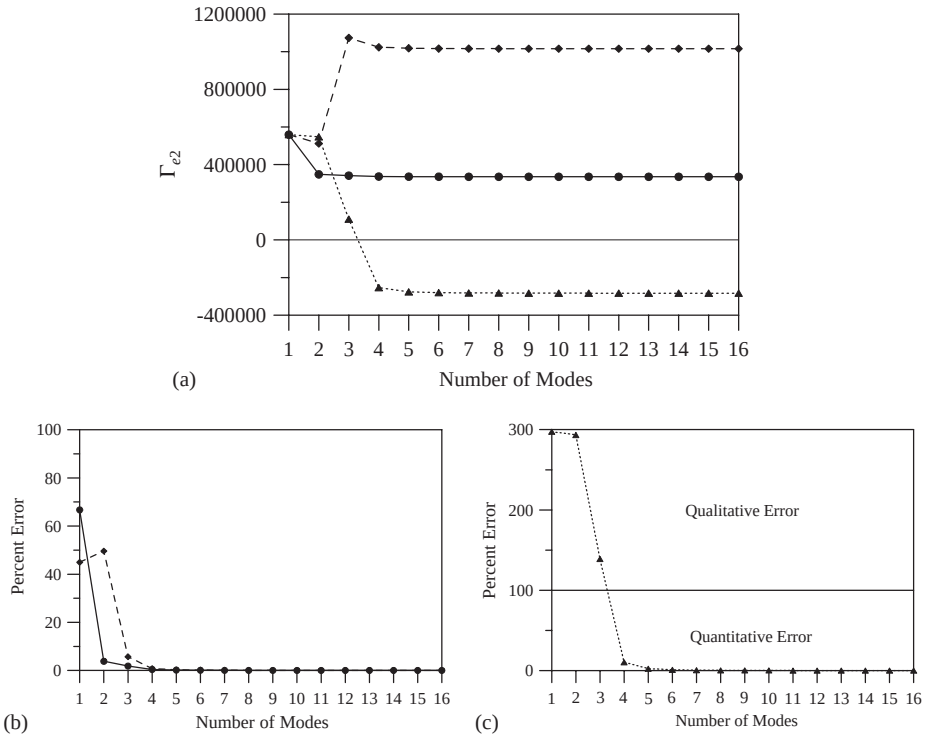

Fig. 7. (a) The coefficient Γ_{e2} of the effective non-linearity of the first antisymmetric in-plane mode and (b), (c) the percent errors as functions of the number modes considered when $\alpha = 239.16$ and $\alpha b^2 = \frac{1}{2}$ (—●—); $\alpha b^2 = 2$ (–◆–), and $\alpha b^2 = 4$ (···▲···).

magnified for values of αb^2 greater than 2 and can be qualitative as well as quantitative. Moreover, the effect of the singularities due to the resonance $\omega_5 \approx 2\omega_1$ is not accounted for in the value of Γ_{e1}. If one uses a three-mode discretization, the values of Γ_{e1} and Γ^*_{e1} seem to match well up to approximately $\alpha b^2 = 5$. Instead, a five-mode discretization seems to give sufficiently good agreement up to $\alpha b^2 = 10$ and possibly more. However, for such large values of αb^2, the shallow suspended cable theory used here may not hold.

5.3.2. First antisymmetric in-plane mode: $\Omega \approx \omega_2$

Next, we use Eq. (77) to calculate Γ_{e2} for the first antisymmetric in-plane mode. In Fig. 7(a), we demonstrate the dependence of Γ_{e2} on the number of modes (including mode 2) retained for the three cases: $\alpha b^2 = \frac{1}{2}$, $\alpha b^2 = 2$, and $\alpha b^2 = 4$. And, in Figs. 7(b) and 7(c), we present the corresponding percent errors. Because, from Eq. (77), the value of Γ_{em} when using a single-mode discretization does not depend on b, in all three cases, Γ_{e2} begins at the same value of 559 112.6.

For the case $\alpha b^2 = \frac{1}{2}$, we find that Γ_{e2} quickly converges to the solution of the direct approach $\Gamma^*_{e2} = 335\,392.4$ as we use more than one mode in the discretization. The relative errors when using single-, two-, three-, and ten-mode discretizations are 66.7%, 3.8%, 1.8%, and 0.013%, as shown in Fig. 7(b). For the case $\alpha b^2 = 2$, the single- and two-mode discretizations give relatively close results. However, when using three or more modes, Γ_{e2} increases significantly, and after retaining 16 modes it approaches $\Gamma^*_{e2} = 1\,015\,797.4$. In this case, the percent errors when using single-, two-, three-, and ten-mode discretizations are 45.0%, 49.6%, 5.7%, and 0.017%, respectively, as shown in Fig. 7(b). In both of these cases, the values of $\Gamma_{e2} > 0$, and therefore the effective non-linearity of the first antisymmetric in-plane mode is hardening.

When $\alpha b^2 = 4$, we find from Fig. 7(a) that $\Gamma_{e2} > 0$ when using single-, two-, and three-mode discretizations. However, using four- or higher-mode discretizations, we find that $\Gamma_{e2} < 0$, and when we retain 16 modes, $\Gamma_{e2} = -283\,281.91$. The corresponding value of $\Gamma^*_{e2} = -283\,357.1$. Therefore, in this case, the error due to single-mode discretization is qualitative as well as quantitative. That is, for this case, the single-mode discretization predicts the effective non-linearity of the first antisymmetric in-plane mode to be hardening, when in fact it is softening.

To further illustrate this point, we show in Fig. 8 typical frequency–response curves when $\alpha b^2 = 4$, $F_{12} = 0.001$, and $\mu_{12} = 0.02$. The curves for the single- and two-mode discretizations indicate a relatively very hardening behavior. However, this hardening behavior significantly diminishes when using a three-mode discretization. And, if a fourth mode is included in the discretization, the frequency–response curves bend to the left, indicating a softening behavior. This softening behavior is also demonstrated by the curves obtained with the direct approach. Furthermore, we show in Fig. 9 typical force–response curves when $\alpha b^2 = 4$, $\sigma = 0.1$, and $\mu_{12} = 0.02$. The curves obtained using single- and two-mode discretizations are quite close to each other. Retaining a third mode, we find that a considerable shift in the saddle-node bifurcations occurs. However, with the inclusion of a fourth mode, the saddle-node bifurcations vanish and the amplitude a_2 becomes monotonously increasing with F_{12}; that is, a characteristic change in the force–response curves, which closely match those obtained with the direct approach, occurs. The percent errors when using single-, two-, three-, four-, and ten-mode discretizations are 297.3%, 293.3%, 138.9%, 10.4%, and 0.13%, respectively, as shown in Fig. 7(c).

The influence of αb^2 on Γ_{e2} is presented in Fig. 10. These same results also apply to the effective non-linearity coefficient Λ_{e2} when the second out-of-plane mode is excited near primary

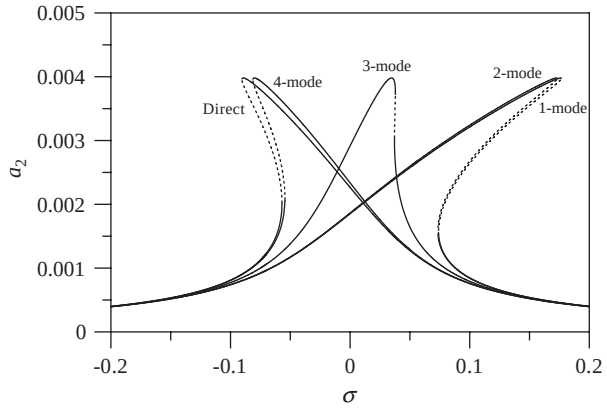

Fig. 8. Typical frequency–response curves for primary resonance of the first antisymmetric in-plane mode when $\alpha b^2 = 4$, $F_{12} = 0.001$, and $\mu_{12} = 0.02$. Solid (—) and dotted (···) lines denote stable and unstable fixed points, respectively.

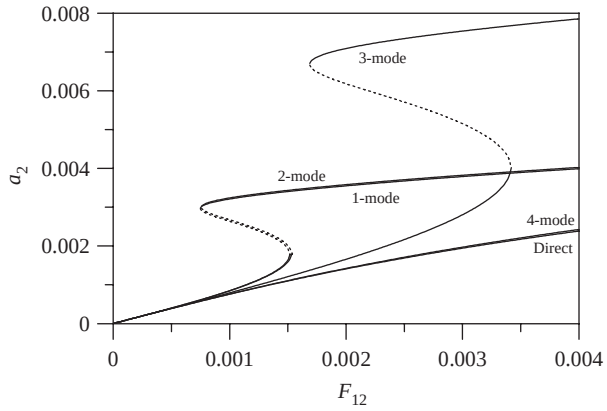

Fig. 9. Typical force–response curves for primary resonance of the first antisymmetric in-plane mode when $\alpha b^2 = 4$, $\sigma = 0.1$, and $\mu_{12} = 0.02$. Solid (—) and dotted (···) lines denote stable and unstable fixed points, respectively.

resonance, as will be discussed in the subsequent section. Results when using the direct and discretization approaches (single-, two-, three-, and five-mode) are presented in Fig. 10. For $\alpha b^2 \in [0, 10]$, the results for Γ_{e2}^* contain a singularity at the second crossover which corresponds to the autoparametric resonance $\omega_3 \approx 2\omega_2$. Similar singularities also occur at the fourth, sixth, etc., crossover points. Using a single-mode discretization, we find that the value of Γ_{e2} remains constant for any value of αb^2. Using a two-mode discretization, we find that Γ_{e2} is sensitive to αb^2 for very shallow suspended cables (e.g., $\alpha b^2 < 1$). However, as αb^2 becomes larger, the results of the two-mode discretization very quickly approach the constant value obtained from the single-mode discretization. Neither of these two discretization approaches take into account the second crossover. The three-mode discretization yields good agreement with the direct approach for up to $\alpha b^2 \approx 2$. However, as with the two-mode discretization, its results also approach the results of the

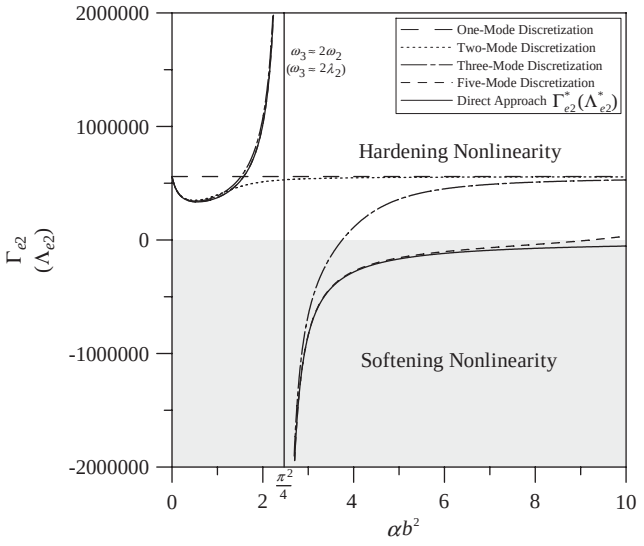

Fig. 10. The coefficient Γ_{e2} (Λ_{e2}) of the effective non-linearity of the first antisymmetric in-plane (out-of-plane) mode as a function of αb^2 when $\alpha = 239.16$.

single-mode discretization for $\alpha b^2 > 3$. Therefore, for results that closely match Γ^*_{e2} over $\alpha b^2 \in [0, 10]$, a five-mode or higher discretization is necessary, as shown in Fig. 10.

6. Primary resonance of an out-of-plane mode

We consider here the cable's response when the mth out-of-plane mode is excited harmonically near primary resonance and assume that it is not involved in an autoparametric resonance with any of the other modes.

6.1. Direct approach

In this case, we set $f_1(T_0) = 0$ and

$$f_2(T_0) = F_2 \cos(\Omega T_0), \tag{80}$$

where Ω is related to λ_m by

$$\Omega = \lambda_m + \varepsilon\sigma. \tag{81}$$

Because the system is damped, the free response of the cable after a long time is given by

$$u_{11}(x, T_0, T_1, T_2) = 0, \tag{82}$$

$$u_{21}(x, T_0, T_1, T_2) = \psi_m(x)[B_m(T_1, T_2)e^{i\lambda_m T_0} + \bar{B}_m(T_1, T_2)e^{-i\lambda_m T_0}]. \tag{83}$$

Substituting Eqs. (82) and (83) into Eqs. (28) and (29), we find that $B_m = B_m(T_2)$ only, $u_{22} = 0$, and

$$D_0^2 u_{12} - u_{12}'' - \alpha b^2 y'' \int_0^1 y' u_{12}' \, \mathrm{d}x = 4\alpha b Q_{mm}[(B_m^2 \mathrm{e}^{2\mathrm{i}\lambda_m T_0} + cc) + 2B_m \bar{B}_m]. \tag{84}$$

The solution of Eqs. (84) and (32) is

$$u_{12}(x, T_0, T_2) = H_1(x)(B_m^2 \mathrm{e}^{2\mathrm{i}\lambda_m T_0} + cc) + H_2(x) B_m \bar{B}_m, \tag{85}$$

where the functions $H_1(x)$ and $H_2(x)$ are governed by the following boundary-value problems:

$$H_1'' + 4\lambda_m^2 H_1 + \alpha b^2 y'' \int_0^1 y' H_1' \, \mathrm{d}x = -4\alpha b Q_{mm}, \quad H_1(0) = H_1(1) = 0, \tag{86}$$

$$H_2'' + \alpha b^2 y'' \int_0^1 y' H_2' \, \mathrm{d}x = -8\alpha b Q_{mm}, \quad H_2(0) = H_2(1) = 0. \tag{87}$$

In Appendix B, we present the solutions of Eqs. (86) and (87).

Next, we substitute Eqs. (83) and (85) into Eq. (31), use Eq. (81), and obtain

$$\begin{aligned} D_0^2 u_{23} - u_{23}'' = & \left\{ -2\mathrm{i}\lambda_m \psi_m \left(\frac{\mathrm{d}B_m}{\mathrm{d}T_2} + c_2 B_m \right) \right. \\ & + \alpha b \left[\psi_m'' \int_0^1 y' H_1' \, \mathrm{d}x + \psi_m'' \int_0^1 y' H_2' \, \mathrm{d}x \right] B_m^2 \bar{B}_m \\ & \left. + \alpha \left(\frac{3}{2} \psi_m'' \int_0^1 \psi_m'^2 \, \mathrm{d}x \right) B_m^2 \bar{B}_m + \frac{1}{2} F_2 \mathrm{e}^{\mathrm{i}\sigma T_2} \right\} \mathrm{e}^{\mathrm{i}\lambda_m T_0} + cc + NST \\ \equiv & \mathscr{H}(x, T_2) \mathrm{e}^{\mathrm{i}\lambda_m T_0} + cc + NST. \end{aligned} \tag{88}$$

Then, letting

$$u_{23}(x, T_0, T_2) = H_3(x, T_2) \mathrm{e}^{\mathrm{i}\lambda_m T_0} + cc + NST \tag{89}$$

in Eqs. (88) and (32), we obtain

$$\frac{\partial^2 H_3}{\partial x^2} + \lambda_m^2 H_3 = -\mathscr{H}(x, T_2), \quad H_3(0) = H_3(1) = 0. \tag{90}$$

The homogeneous problem in Eq. (90) has non-trivial solutions, and therefore the non-homogeneous problem has solutions provided that a solvability condition is satisfied. To this end, we multiply Eq. (90) by the adjoint function $h_3(x)$, integrate the outcome by parts from $x = 0$ to 1, and obtain

$$\left[h_3 \frac{\partial H_3}{\partial x} \right]_0^1 + \int_0^1 H_3 (h_3'' + \lambda_m^2 h_3) \, \mathrm{d}x = -\int_0^1 h_3 \mathscr{H} \, \mathrm{d}x. \tag{91}$$

Following the same procedure used in Section 5.1, we find that the adjoint $h_3(x) = \psi_m(x)$ and consequently, the solvability condition is given by

$$\int_0^1 \psi_m(x) \mathscr{H}(x, T_2) \, \mathrm{d}x = 0. \tag{92}$$

Then, from Eqs. (18), (88), and (92), we obtain the following equation for $B_m(T_2)$:

$$2\mathrm{i}\lambda_m\left(\frac{\mathrm{d}B_m}{\mathrm{d}T_2}+\mu_{2m}B_m\right)+\Lambda^*_{em}B_m^2\bar{B}_m=\frac{1}{2}F_{2m}\mathrm{e}^{\mathrm{i}\sigma T_2}, \tag{93}$$

where $F_{2m}=\int_0^1 F_2\psi_m\,\mathrm{d}x$ and the coefficient Λ^*_{em} of the effective non-linearity for the mth out-of-plane mode is given by

$$\begin{aligned}\Lambda^*_{em}&=\frac{3}{2}\alpha Q_{mm}^2+\alpha bQ_{mm}\int_0^1 y'(H_1'+H_2')\,\mathrm{d}x\\&=\frac{3}{2}\alpha m^4\pi^4-\frac{8\alpha^2b^2m^4\pi^4(48\alpha b^2+3-2m^2\pi^2)}{(16\alpha b^2+3)(16\alpha b^2-m^2\pi^2)},\quad m=1,2,3,\ldots\ .\end{aligned} \tag{94}$$

We note from Eq. (94) that the solution becomes nonuniform when $\lambda_m^2=m^2\pi^2\approx 16\alpha b^2$; that is, near the mth crossover. In addition, the overall response of the cable is given by

$$u_1(x,t)=\tfrac{1}{2}\varepsilon^2\hat{a}_m^2[H_1(x)\cos(2\lambda_m t+2\hat{\beta}_m)+\tfrac{1}{2}H_2(x)]+O(\varepsilon^3), \tag{95}$$

$$u_2(x,t)=\varepsilon\psi_m(x)\hat{a}_m\cos(\lambda_m t+\hat{\beta}_m)+O(\varepsilon^3). \tag{96}$$

Therefore, even though only the mth out-of-plane mode is directly excited and there is no autoparametric resonance between it and any other mode, the motion of the cable has a non-trivial component in the in-plane direction. This is a direct consequence of the sag in the cable.

6.2. Discretization approach

Here, we set

$$\eta_{k1}=0\quad\forall k, \tag{97}$$

$$\zeta_{m1}=B_m(T_1,T_2)\mathrm{e}^{\mathrm{i}\lambda_m T_0}+cc, \tag{98}$$

$$\zeta_{l1}=0\quad\forall l\neq m, \tag{99}$$

$$f_{1k}(T_0)=0\quad\forall k, \tag{100}$$

$$f_{2l}(T_0)=F_{2l}\cos(\Omega T_0)\quad\forall l, \tag{101}$$

where Ω is related to λ_m by Eq. (81). We substitute Eqs. (97)–(99) into Eqs. (40) and (41), set $\partial B_m/\partial T_1=0$, solve for the η_{k2} and ζ_{l2}, and obtain

$$\eta_{k2}=E_{3k}(B_m^2\mathrm{e}^{2\mathrm{i}\lambda_m T_0}+cc)+E_{4k}B_m\bar{B}_m\quad\forall k, \tag{102}$$

$$\zeta_{l2}=0\quad\forall l, \tag{103}$$

where

$$E_{3k}=\frac{1}{2}\alpha b\left(\frac{U_kQ_{mm}}{\omega_k^2-4\lambda_m^2}\right)\quad\text{and}\quad E_{4k}=\alpha b\left(\frac{U_kQ_{mm}}{\omega_k^2}\right). \tag{104}$$

It follows from Eqs. (102) and (104) that this expansion is non-uniform if $\omega_k\approx 2\lambda_m$, corresponding to the mth crossover. This case of two-to-one autoparametric resonance between an in-plane

mode and an out-of-plane mode was investigated by Visweswara Rao and Iyengar [17], Lee and Perkins [18], and Perkins [19] for different excitation conditions. In all three cases, the method of multiple scales was applied to a set of non-linear ordinary-differential equations which were obtained from a two-mode Galerkin discretization procedure.

Noting that near crossover points, the one-to-one autoparametric resonances $\omega_{2k-1} \approx \omega_{2k} = \lambda_{2k}$ also exist, Benedettini and Rega [20], Benedettini et al. [21], Lee and Perkins [22], Rega et al. [23], and Nayfeh et al. [13] investigated the influence of the simultaneous autoparametric resonances $\omega_1 \approx 2\lambda_1 = \omega_2 = \lambda_2$ on the responses of suspended cables for different excitation conditions. In the first three works [20–22], the authors applied the method of multiple scales to a set of non-linear ordinary-differential equations which were obtained from a four-mode Galerkin discretization procedure. In the last two works [23,13], the authors applied the method of multiple scales directly to the governing partial-differential system.

Next, we substitute Eqs. (97), (99), (101), and (103) into Eq. (43), set $l = m$, and obtain the following equation for ζ_{m3}:

$$D_0^2\zeta_{m3} + \lambda_m^2\zeta_{m3} = -2D_0D_2\zeta_{m1} - 2\mu_{2m}D_0\zeta_{m1} - \frac{1}{2}\alpha Q_{mm}^2\zeta_{m1}^3 + \alpha b\sum_{r=1}^{\infty}[(Q_{mm}U_r)\zeta_{m1}\eta_{r2}] + F_{2m}\cos(\Omega T_0). \tag{105}$$

Then, substituting for ζ_{m1} and η_{k2} from Eqs. (98) and (102) into Eq. (105), using Eq. (81), and setting the terms that produce secular terms equal to zero, we obtain the following equation for $B_m(T_2)$:

$$2\mathrm{i}\lambda_m\left(\frac{\mathrm{d}B_m}{\mathrm{d}T_2} + \mu_{2m}B_m\right) + \Lambda_{em}B_m^2\bar{B}_m = \frac{1}{2}F_{2m}\mathrm{e}^{\mathrm{i}\sigma T_2}, \tag{106}$$

where $m = 1, 2, 3, \ldots$. The coefficient Λ_{em} of the effective non-linearity of the mth out-of-plane mode is given by

$$\Lambda_{em} = \frac{3}{2}\alpha Q_{mm}^2 - \frac{1}{2}\alpha^2 b^2\sum_{r=1}^{\infty}\left\{(Q_{mm}U_r)^2\left[\frac{3\omega_r^2 - 8\lambda_m^2}{\omega_r^2(\omega_r^2 - 4\lambda_m^2)}\right]\right\}. \tag{107}$$

Substituting for the U_r, Q_{mm}, and λ_m, we reduce Eq. (107) to the following:

$$\Lambda_{em} = \frac{3}{2}\alpha m^4\pi^4 - \frac{m^4\pi^4}{128b^2}\sum_{r=odd}^{\infty}\left[\frac{\kappa_r^2\omega_r^2(3\omega_r^2 - 8m^2\pi^2)}{(\omega_r^2 - 4m^2\pi^2)}\right] \quad \forall m. \tag{108}$$

The corresponding solution for the response of the cable is

$$u_1(x,t) = \frac{1}{2}\varepsilon^2\hat{a}_m^2\sum_{r=odd}^{\infty}\left\{\phi_r(x)\left[E_{3r}\cos(2\lambda_r t + 2\hat{\beta}_r) + \frac{1}{2}E_{4r}\right]\right\} + O(\varepsilon^3), \tag{109}$$

$$u_2(x,t) = \varepsilon\psi_m(x)\hat{a}_m\cos(\lambda_m t + \hat{\beta}_m) + O(\varepsilon^3). \tag{110}$$

Comparing Eqs. (109) and (110) with Eqs. (95) and (96), we find that the solutions from the discretization and direct approaches match if $\sum_{r=odd}^{\infty} E_{3r}\phi_r(x) = H_1(x)$ and $\sum_{r=odd}^{\infty} E_{4r}\phi_r(x) = H_2(x)$.

6.3. Results and comparison

We note that if $\Lambda_{em}, \Lambda^*_{em} > 0$, then the effective non-linearity of the mth out-of-plane mode is of the "hardening" type and if $\Lambda_{em}, \Lambda^*_{em} < 0$, then the effective non-linearity of the mth out-of-plane mode is of the "softening" type. In addition, Eqs. (94) and (108) are the same as the expressions we have obtained for Γ^*_{em} and Γ_{em} when the mth antisymmetric in-plane mode is excited near primary resonance. Therefore, the results of Figs. 7 and 10, which we have discussed in Section 5 for Γ_{e2}, also apply to Λ_{e2} (i.e., primary resonance of the second out-of-plane mode).

Consequently, we consider here the primary resonance of the first out-of-plane mode and present in Fig. 11 results for the three cases: $\alpha b^2 = \frac{1}{2}$ (left of first crossover), $\alpha b^2 = 2$ (right of first crossover), and $\alpha b^2 = 4$ (right of second crossover), where we take $\alpha = 239.16$. In all three cases, the value of $\Lambda_{e1} = 34\,944.5$ when using a single-mode discretization.

When $\alpha b^2 = \frac{1}{2}$, the value of Λ_{e1} jumps up to 70 841.0 when we use a two-mode discretization. Retaining more modes in the discretization, the value of Λ_{e1} quickly approaches the value obtained from the direct approach $\Lambda^*_{e1} = 67\,844.1$. Replacing Γ by Λ in Eq. (79), we calculate the relative errors when using single-, two-, three-, and ten-mode discretizations as 48.5%, 4.4%, 0.4%, and 0.004%, respectively, as shown in Fig. 12(a).

Taking $\alpha b^2 = 2$, we find that when we use a two-mode discretization, Λ_{e1} drops to 24 300.7. Using a three-mode discretization, Λ_{e1} drops even further to -605.3. Continuing to add more modes in the discretization, we find that Λ_{e1} approaches $\Lambda^*_{e1} = -3198.0$. The percent errors for single-, two-, three-, and ten-mode discretizations are 1192.7%, 859.9%, 81.1%, and 0.34% (Fig. 12(b)), which indicate very significant quantitative discrepancies when using three modes or less in the discretization. More importantly, the errors in this case are also qualitative, indicating a hardening effective non-linearity when in fact it is softening.

Overall, the results for $\alpha b^2 = 4$ are similar to the previous case. Using four modes or less in the discretization, the effective non-linearity is predicted to be hardening, whereas, in fact, it is softening, as indicated by the direct approach result $\Lambda^*_{e1} = -1080.7$. The percent errors when

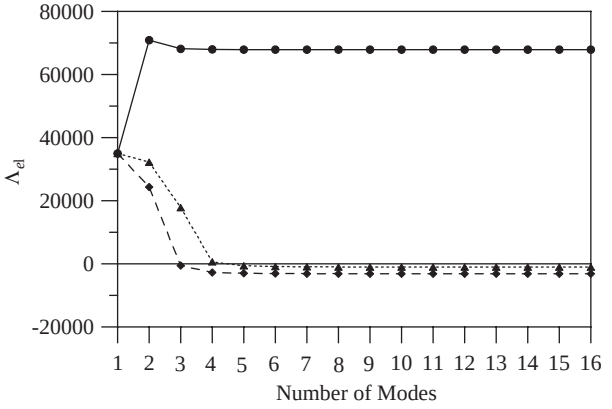

Fig. 11. The coefficient Λ_{e1} of the effective non-linearity of the first out-of-plane mode as a function of the number modes retained in the discretization when $\alpha = 239.16$ and the cases $\alpha b^2 = \frac{1}{2}$ (—●—), $\alpha b^2 = 2$ (–◆–), and $\alpha b^2 = 4$ (···▲···).

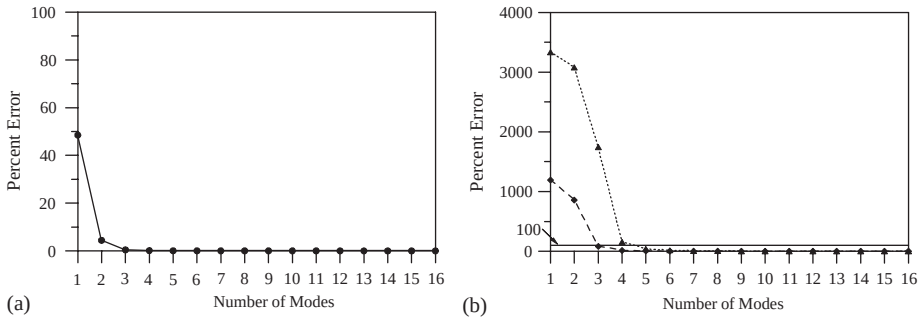

Fig. 12. The percent error in calculating Λ_{e1} in Fig. 11 as a function of the number modes considered when $\alpha = 239.16$. In part (a) $\alpha b^2 = \frac{1}{2}$ (—●—) and in part (b) $\alpha b^2 = 2$ (–◆–) and $\alpha b^2 = 4$ (···▲···).

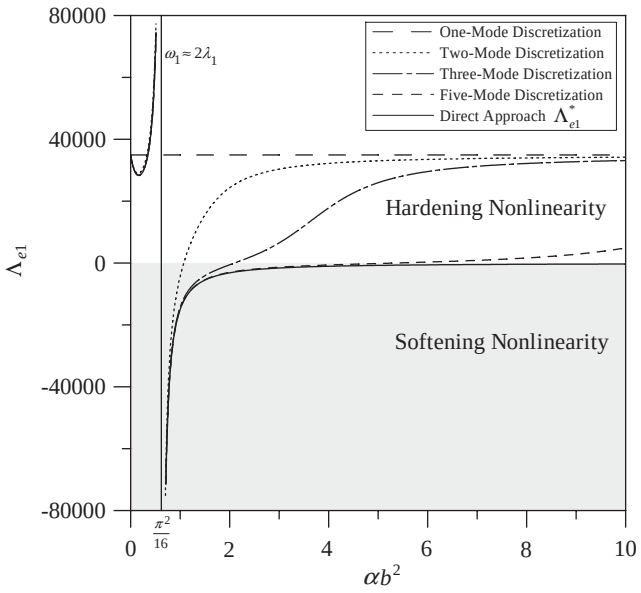

Fig. 13. The coefficient Λ_{e1} of the effective non-linearity of the first out-of-plane mode as a function of αb^2 when $\alpha = 239.16$.

using single-, two-, three-, four-, five-, and ten-mode discretizations are 3333.5%, 3078.5%, 1745.1%, 153.76%, 38.0%, and 2.1%, respectively (Fig. 12(b)). These values emphasize the need to include a sufficiently large number of modes in the discretization in order to obtain accurate results.

In Fig. 13, we show the influence of αb^2 on Λ_{e1} when using the direct and discretization approaches. Results for single-, two-, three-, and five-mode discretizations are included. The results for Λ^*_{e1} contain a singularity for $\alpha b^2 = \pi^2/16$; this corresponds to the two-to-one autoparametric resonance $\omega_1 \approx 2\lambda_1$ which occurs at the first crossover.

The single-mode discretization results in Fig. 13 are constant over αb^2, and hence do not account for this singularity. Using two-mode or three-mode discretizations, we find relatively good agreement with

the results of the direct approach when $\alpha b^2 < 0.5$. However, for larger values of αb^2, the results from these two discretizations deviate from Λ_{e1}^* and tend to the result of the single-mode discretization. The five-mode discretization yields good agreement with Λ_{e1}^* but also loses some accuracy for $\alpha b^2 > 6$, indicating more modes should be retained in the discretization for large values of αb^2.

7. Summary

We investigated the non-linear responses of shallow suspended cables to primary resonance excitations and considered both in-plane and out-of-plane motions. We assumed that the directly excited mode is not involved in an autoparametric resonance with any of the other modes and used the method of multiple scales to obtain second-order approximations of the solutions. To this end, we followed two approaches. In the first, we applied the method of multiple scales directly to the partial-differential equations of motion and associated boundary conditions (direct approach). In the second, we applied the method of multiple scales to a set of non-linear ordinary-differential equations, which were obtained by the Galerkin discretization procedure (discretization approach).

We investigated the influence of the number of terms retained in the discretization procedure on the accuracy of the predicted effective non-linearity, and hence the cable response. We found out that in all cases, only the symmetric in-plane modes contribute to the effective non-linearity. We also compared the solutions obtained from the direct and discretization approaches and presented results for the following cases: (a) $\Omega \approx \omega_1$ (b) $\Omega \approx \omega_2$ (c) $\Omega \approx \lambda_1$ and (d) $\Omega \approx \lambda_2$. We found out that using a single-mode discretization can lead to significant quantitative errors in estimating the value of the effective non-linearity. In some cases, two- and three-mode discretizations can lead to as much errors as a single-mode discretization. Moreover, we found out that a single-mode discretization may result in qualitative errors by predicting that the effective non-linearity is hardening, when in fact it is softening. In all cases, however, the solutions converge onto the direct approach solutions once enough modes are retained in the discretization procedure.

Appendix A. Calculating the functions $G_1(x)$ and $G_2(x)$

The functions $G_1(x)$ and $G_2(x)$ are governed by Eqs. (53) and (54). Depending on the type of the in-plane mode being excited (symmetric or antisymmetric), different solutions are obtained.

A.1. Primary resonance of a symmetric in-plane mode

For primary resonance of the mth symmetric in-plane mode, Eq. (53) becomes

$$G_1'' + 4\omega_m^2 G_1 = \alpha b(c_1 - 4P_{mm}) + \alpha b\kappa_m \omega_m^2 U_m \cos(\omega_m x) + \alpha b\kappa_m \omega_m^2 U_m \tan\left(\frac{\omega_m}{2}\right)\sin(\omega_m x), \tag{A.1}$$

where c_1 is a constant defined as

$$c_1 = -by'' \int_0^1 y' G_1' \, \mathrm{d}x = 32b \int_0^1 (1 - 2x) G_1' \, \mathrm{d}x. \tag{A.2}$$

The general solution of Eq. (A.1) is

$$G_1(x) = a_1 \sin(2\omega_m x) + a_2 \cos(2\omega_m x) + d_1 + d_2 \sin(\omega_m x) + d_3 \cos(\omega_m x), \tag{A.3}$$

where

$$d_1 = \frac{\alpha b(c_1 - 4P_{mm})}{4\omega_m^2}, \quad d_2 = R_m \tan\left(\frac{\omega_m}{2}\right), \quad d_3 = R_m \tag{A.4}$$

and

$$R_m \equiv \tfrac{1}{3}\alpha b \kappa_m U_m. \tag{A.5}$$

Next we apply the boundary conditions $G_1(0) = G_1(1) = 0$ and obtain

$$a_1 = \frac{(d_1 + d_3)\cos(2\omega_m) - d_1 - d_2 \sin\omega_m - d_3 \cos\omega_m}{\sin(2\omega_m)}, \quad a_2 = -(d_1 + d_3). \tag{A.6}$$

Then, we substitute Eq. (A.3) into Eq. (A.2), solve for c_1, and substitute the result back into the first of Eqs. (A.4) to get the following final expression for d_1:

$$d_1 = \frac{\alpha b[\omega_m P_{mm} \cos\omega_m + 32 b R_m \tan(\frac{\omega_m}{2}) \sin^2(\frac{\omega_m}{2})]}{\cos\omega_m[16\alpha b^2(\omega_m - \tan\omega_m) - \omega_m^3]}. \tag{A.7}$$

Similarly, Eq. (54) for $G_2(x)$ reduces to

$$\begin{aligned} G_2'' = {} & \alpha b(c_2 - 8P_{mm}) + 2\alpha b \kappa_m \omega_m^2 U_m \cos(\omega_m x) \\ & + 2\alpha b \kappa_m \omega_m^2 U_m \tan\left(\frac{\omega_m}{2}\right) \sin(\omega_m x), \end{aligned} \tag{A.8}$$

where

$$c_2 = -by'' \int_0^1 y' G_2' \, \mathrm{d}x = 32b \int_0^1 (1 - 2x) G_2' \, \mathrm{d}x. \tag{A.9}$$

The solution of Eq. (A.8) is given by

$$G_2(x) = a_3 + a_4 x + d_4 x^2 + d_5 \sin(\omega_m x) + d_6 \cos(\omega_m x), \tag{A.10}$$

where

$$d_4 = \frac{1}{2}\alpha b(c_2 - 8P_{mm}), \quad d_5 = -6R_m \tan\left(\frac{\omega_m}{2}\right), \quad d_6 = -6R_m. \tag{A.11}$$

Applying the boundary conditions $G_2(0) = G_2(1) = 0$, we obtain

$$a_3 = -d_6 \quad \text{and} \quad a_4 = (d_6 - d_4) - d_5 \sin\omega_m - d_6 \cos\omega_m. \tag{A.12}$$

Substituting Eq. (A.10) into Eq. (A.9), solving for c_2, and then substituting the result into the first of Eqs. (A.11), we obtain the following final expression for d_4:

$$d_4 = -\frac{3(4\alpha b P_{mm} - 3\omega_m^2 R_m)}{(16\alpha b^2 + 3)}. \tag{A.13}$$

A.2. Primary resonance of an antisymmetric in-plane mode

For primary resonance of the mth antisymmetric in-plane mode, we set $U_m = 0$ in Eq. (53) and obtain

$$G_1'' + 4\omega_m^2 G_1 + \alpha b^2 y'' \int_0^1 y' G_1' \, \mathrm{d}x = -4\alpha b P_{mm}. \tag{A.14}$$

Eq. (A.14) can be rewritten as

$$G_1'' + 4\omega_m^2 G_1 = \alpha b(c_1 - 4P_{mm}), \tag{A.15}$$

where c_1 is defined by Eq. (A.2). The solution of Eq. (A.15) is given by

$$G_1(x) = a_5 \sin(2\omega_m x) + a_6 \cos(2\omega_m x) + d_7, \tag{A.16}$$

where

$$d_7 = \frac{\alpha b(c_1 - 4P_{mm})}{4\omega_m^2}. \tag{A.17}$$

Using the boundary condition $G_1(0) = 0$, we obtain $a_6 = -d_7$. In this case, however, the second boundary condition $G_1(1) = 0$ yields the same condition on a_6, and hence a_5 remains unknown. To determine a_5 and render the solution unique, we require that the solution $G_1(x)$ be orthogonal to the adjoint function $g_1(x)$. To this end, we multiply Eq. (A.14) by $g_1(x)$, integrate by parts from $x = 0$ to 1, and obtain

$$\begin{aligned} &\left[g_1 G_1' - \alpha b^2 g_1 y' \left(\int_0^1 y'' G_1 \, \mathrm{d}x \right) \right]_0^1 + \int_0^1 G_1 \left[g_1'' + 4\omega_m^2 g_1 + \alpha b^2 y'' \int_0^1 g_1' y' \, \mathrm{d}x \right] \mathrm{d}x \\ &\quad = -4\alpha b P_{mm} \int_0^1 g_1 \, \mathrm{d}x. \end{aligned} \tag{A.18}$$

Then, we solve the homogeneous problem in Eq. (A.18) and obtain $g_1(x) = \sqrt{2}\sin(2\omega_m x)$. Consequently, the constraint $\int_0^1 g_1 G_1 \, \mathrm{d}x = 0$ yields $a_5 = 0$. Next, we substitute Eq. (A.16) into Eq. (A.2), solve for c_1, determine d_7 from Eq. (A.17), and obtain the final expression for $G_1(x)$ as

$$G_1(x) = \frac{\alpha b P_{mm}}{16\alpha b^2 - \omega_m^2}[1 - \cos(2\omega_m x)]. \tag{A.19}$$

To determine $G_2(x)$, we set $U_m = 0$ in Eq. (54) and obtain

$$G_2'' = \alpha b(c_2 - 8P_{mm}), \tag{A.20}$$

where c_2 is defined by Eq. (A.9). The solution of Eq. (A.20) is equal to

$$G_2(x) = a_7 + a_8 x + \tfrac{1}{2}\alpha b(c_2 - 8P_{mm})x^2. \tag{A.21}$$

Using the boundary conditions $G_2(0) = G_2(1) = 0$ to determine a_7 and a_8 and then substituting the results into Eq. (A.9) to determine c_2, we obtain the following final expression for $G_2(x)$:

$$G_2(x) = -\frac{12\alpha b P_{mm}}{16\alpha b^2 + 3}(x^2 - x). \tag{A.22}$$

Appendix B. Calculating the functions $H_1(x)$ and $H_2(x)$

The function $H_1(x)$ is governed by Eq. (86), which we rewrite as

$$H_1'' + 4\lambda_m^2 H_1 = (c_3 - 4\alpha b Q_{mm}), \tag{B.1}$$

where

$$c_3 = -\alpha b^2 y'' \int_0^1 y' H_1' \, \mathrm{d}x. \tag{B.2}$$

Using the boundary conditions $H_1(0) = H_1(1) = 0$, the solution of Eq. (B.1) is

$$H_1(x) = a_9 \sin(2\lambda_m x) + \frac{(c_3 - 4\alpha b Q_{mm})}{4\lambda_m^2}[1 - \cos(2\lambda_m x)]. \tag{B.3}$$

Then, substituting Eq. (B.3) into Eq. (B.2) and solving for c_3, the expression for $H_1(x)$ becomes

$$H_1(x) = a_9 \sin(2\lambda_m x) + \frac{\alpha b Q_{mm}}{(16\alpha b^2 - \lambda_m^2)}[1 - \cos(2\lambda_m x)]. \tag{B.4}$$

To calculate a_9 and determine a unique solution, we require that the solution $H_1(x)$ be orthogonal to the adjoint function $h_1(x)$. To determine the adjoint, we multiply Eq. (86) by $h_1(x)$, integrate by parts from $x = 0$ to 1, and obtain

$$\left[h_1 H_1' - \alpha b^2 h_1 y' \left(\int_0^1 y'' H_1 \, \mathrm{d}x\right)\right]_0^1 + \int_0^1 H_1 \left[h_1'' + 4\lambda_m^2 h_1 + \alpha b^2 y'' \int_0^1 h_1' y' \, \mathrm{d}x\right] \mathrm{d}x$$
$$= -4\alpha b Q_{mm} \int_0^1 h_1 \, \mathrm{d}x. \tag{B.5}$$

Then, we solving the homogeneous problem in Eq. (B.5) and obtain $h_1(x) = \sqrt{2}\sin(2\lambda_m x)$. Consequently, the constraint $\int_0^1 h_1 H_1 \, \mathrm{d}x = 0$ yields $a_9 = 0$, and therefore the final expression for $H_1(x)$ is

$$H_1(x) = \frac{\alpha b Q_{mm}}{(16\alpha b^2 - \lambda_m^2)}[1 - \cos(2\lambda_m x)]. \tag{B.6}$$

The function $H_2(x)$ is governed by Eq. (87), which we rewrite as

$$H_2'' = (c_4 - 8\alpha b Q_{mm}), \tag{B.7}$$

where

$$c_4 = -\alpha b^2 y'' \int_0^1 y' H_2' \, \mathrm{d}x. \tag{B.8}$$

Integrating Eq. (B.7) twice, using the boundary conditions $H_2(0) = H_2(1) = 0$, and then substituting the result into Eq. (B.8) to determine c_4, we obtain the final expression for $H_2(x)$ as

$$H_2(x) = \frac{12\alpha b Q_{mm}}{(16\alpha b^2 + 3)}(x - x^2). \tag{B.9}$$

References

[1] A.H. Nayfeh, J.F. Nayfeh, D.T. Mook, On methods for continuous systems with quadratic and cubic nonlinearities, Nonlinear Dynamics 3 (1992) 145–162.
[2] M. Pakdemirli, S.A. Nayfeh, A.H. Nayfeh, Analysis of one-to-one autoparametric resonances in cables—discretization vs. direct treatment, Nonlinear Dynamics 8 (1995) 65–83.
[3] A.H. Nayfeh, On the discretization of weakly nonlinear spatially continuous systems, in: N.H. Ibragimov, F.M. Mahomed, D.P. Mason, D. Sherwell (Eds.), Differential Equations and Chaos, New Age International Limited, New Delhi, 1997, pp. 3–39.
[4] A.H. Nayfeh, W. Lacarbonara, On the discretization of distributed-parameter systems with quadratic and cubic nonlinearities, Nonlinear Dynamics 13 (1997) 203–220.
[5] A.H. Nayfeh, W. Lacarbonara, On the discretization of spatially continuous systems with quadratic and cubic nonlinearities, JSME International Journal Series C 41 (1998) 510–531.
[6] H.N. Arafat, A.H. Nayfeh, Nonlinear bending-torsion oscillations of cantilever beams to combination parametric excitations, in: Proceedings of the 17th International Modal Analysis Conference, IMAC XVII, Orlando, FL, 1999, pp. 1203–1209.
[7] G. Rega, W. Lacarbonara, A.H. Nayfeh, Reduction methods for nonlinear vibrations of spatially continuous systems with initial curvature, in: Proceedings of the IUTAM Symposium on Recent Developments in Non-Linear Oscillations of Mechanical Systems, Hanoi, Vietnam, 1999, pp. 235–246.
[8] K.A. Alhazza, A.H. Nayfeh, Nonlinear vibrations of doubly-curved cross-ply shallow shells, in: Proceedings of the 42nd AIAA/ASME/ASCE/AHS/ASC Structures, Structural Dynamics, and Materials Conference and Exhibit, Seattle, WA, AIAA Paper# 2001-1661, 2001.
[9] M. Pakdemirli, H. Boyaci, Comparison of direct-perturbation methods with discretization-perturbation methods for non-linear vibrations, Journal of Sound and Vibration 186 (1995) 837–845.
[10] F. Benedettini, G. Rega, Non-linear dynamics of an elastic cable under planar excitation, International Journal of Non-Linear Mechanics 22 (1987) 497–509.
[11] K. Takahashi, Y. Konishi, Non-linear vibrations of cables in three dimensions, Part II: out-of-plane vibrations under in-plane sinusoidally time-varying load, Journal of Sound and Vibration 118 (1987) 85–97.
[12] A.H. Nayfeh, Nonlinear Interactions, Wiley, New York, 2000.
[13] A.H. Nayfeh, H.N. Arafat, C. Chin, W. Lacarbonara, Multimode interactions in suspended cables, Journal of Vibration and Control 8 (2002) 337–387.
[14] H.M. Irvine, T.K. Caughey, The linear theory of free vibrations of a suspended cable, in: Proceedings of the Royal Society of London Series A 341 (1974) 299–315.
[15] A.H. Nayfeh, Introduction to Perturbation Techniques, Wiley, New York, 1981.
[16] A.H. Nayfeh, D.T. Mook, Nonlinear Oscillations, Wiley, New York, 1979.
[17] G. Visweswara Rao, R.N. Iyengar, Internal resonance and non-linear response of a cable under periodic excitation, Journal of Sound and Vibration 149 (1991) 25–41.
[18] C.L. Lee, N.C. Perkins, Nonlinear oscillations of suspended cables containing a two-to-one internal resonance, Nonlinear Dynamics 3 (1992) 465–490.
[19] N.C. Perkins, Modal interactions in the non-linear response of elastic cables under parametric/external excitation, International Journal of Non-Linear Mechanics 27 (1992) 233–250.
[20] F. Benedettini, G. Rega, Analysis of finite oscillations of elastic cables under internal/external resonance conditions, in: Proceedings of the International Mechanical Engineering Congress and Exposition, AMD-Vol. 192/DE-Vol. 78, Chicago, IL, 1994, pp. 39–46.
[21] F. Benedettini, G. Rega, R. Alaggio, Non-linear oscillations of a four-degree-of-freedom model of a suspended cable under multiple internal resonance conditions, Journal of Sound and Vibration 182 (1995) 775–798.
[22] C.L. Lee, N.C. Perkins, Three-dimensional oscillations of suspended cables involving simultaneous internal resonances, Nonlinear Dynamics 8 (1995) 45–63.
[23] G. Rega, W. Lacarbonara, A.H. Nayfeh, C.M. Chin, Multiple resonances in suspended cables: direct versus reduced-order models, International Journal of Non-Linear Mechanics 34 (1999) 901–924.